Energy, Volume 242, March 2022, Article number 122948
DOI:10.1016/j.energy.2021.122948

Experimental Assessment of a Pilot Scale Hybrid Cooling System for Water Consumption Reduction in CSP Plants

Patricia Palenzuela[1,*], Lidia Roca[1,4], Faisal Asfand[2], Kumar Patchigolla[3]

[1]CIEMAT-Plataforma Solar de Almería. Ctra.de Senés s/n, 04200 Tabernas, Almería, Spain.

[2]The School of Computing and Engineering, University of Huddersfield, Huddersfield, HD1 3DH, UK

[3]Centre for Thermal Energy and Materials, School of Water Energy and Environment, Cranfield University, Cranfield, Bedfordshire MK43 0AL, UK

[4]Centro Mixto CIESOL, Universidad de Almería, Ctra. Sacramento s/n, Almería 04120, Spain

[*]Corresponding author, patricia.palenzuela@psa.es, Tel.: +34 950 387800. Ext. 909

Abstract

The new challenge of the European Commission is to limit water consumption in Concentrating Solar Power (CSP) plants, especially significant in the cooling process. Hybrid cooling systems are presented as a potential solution to achieve water consumption reduction since they also avoid a high penalty of efficiency loss in the power block. In this work, a hybrid cooling pilot plant installed at Plataforma Solar de Almería is evaluated experimentally. The system has been tested under different ambient and operating conditions to analyze their influence on the water and electricity consumption. The results revealed that significant water savings were achieved in comparison with the conventional only-wet configuration. Concretely, a maximum water consumption saving of 67% was found at high ambient temperatures (between 25 and 30 ºC) and for a thermal load of 80% when a hybrid configuration was used. The optimal operating strategies that achieve a tradeoff between low water and electricity consumption have been identified by two efficiency indexes: the specific electricity and water consumption. The parallel configuration resulted the optimal one in most of the cases. At high ambient temperatures and 80% thermal load, the electricity and water consumptions of this configuration were 0.033 kW_e/kW_{th} and 0.071 L/kW_{th}, respectively.

Keywords: Hybrid Cooling, Pilot Plant, Water Consumption Saving, Experimental Characterization, Optimal operating strategies

1. Introduction

Water consumption in Concentrating Solar Power (CSP) plants can reach values of up to 3000 m^3/GW_e [1]. These plants are usually implemented in those locations with high Direct Normal Irradiance but at the same time with a significant water scarcity, so it is of extreme importance to reduce their water consumption. The condensation of the exhaust steam is the main source of water consumption and it can be addressed by dry or wet cooling method. Wet cooling

is accomplished using two methods: once-through or evaporative wet cooling. Once-through uses cold water, usually from the sea, so it allows relatively low condensation temperatures, being one of the most preferred refrigeration methods in terms of thermal efficiency of the power cycle. However, its main drawback is the large volume of water that it uses and the pollution threat to aquatic life due to the seawater extraction process and to the return of seawater at a higher temperature [2]. Evaporative wet cooling is the most frequent method in CSP plants since it relies on the wet bulb temperature and thus, leads to higher efficiency of the power block. Its main problem is the requirement of a constant supply of fresh water due to the water evaporation, which is more aggravated in arid regions [3]. An example of the water consumption is provided by a wet-cooled CSP plant located in the Mojave Desert, California, which consumes about 3 m^3/MWh [1]. This high amount of water makes CSP plants unsustainable. Another problem of this kind of cooling systems is the visible plume that is generated when the saturated exhaust air from the wet cooling tower (WCT) mixes with dry and cold ambient air, especially in winter ([4–7]). It induces phenomena like fog, corrosion, moisture and darkness in the surrounding area that contribute to social concerns and, in the case of CSP plants, to a possible decrease in the optical efficiency of the solar collector mirrors closest to the cooling tower.

Dry cooling systems rely on dry bulb temperature and such plants have little or no water consumption. The water consumption in a dry-cooled CSP plant can be reduced to about 95% compared to wet cooling systems (having consumptions of about 0.30-0.34 m^3/MWh [8]). The typical ones are the Air Cooled Condensers (ACC) although there is an improved version of this technology called Air Cooler Heat Exchanger (ACHE). In comparison with ACC, a power plant with ACHE can produce 1% more electricity per year than the same plant with an ACC system [9]. The main drawback of dry cooling systems is the higher capital costs and their significant reduction in the power output (up to 10% [1]) due to the higher condensation temperature required compared to wet cooling systems and to the high electricity consumption by the operation of the fans, especially at high ambient temperatures. Many efforts have been made to increase the efficiency of dry cooling systems to the level of wet cooling systems [10], but still there is a small percentage of these systems installed at CSP plants.

Several studies about the comparison between dry and wet cooling systems in CSP plants can be found in the literature. Poullikas et al. [11] presented a comparative overview of evaporative WCTs and ACC for the Rankine cycle of CSP plants. The comparison was performed considering the overall plant's water requirements, the plant's efficiency, the plant's capital cost and the plant's electricity unit cost. The authors concluded that, although ACC systems offer significant reductions in water consumption against WCTs, their integration results in the overall plant's efficiency reduction between 1-5% and increase in the overall capital costs ranging from 1% to

4%. This could lead to an increase in the net electricity unit cost between 2% and 9%, depending on the CSP technology. Blanco-Marigorta et al. [12] also carried out a comparison between dry and wet cooling technology for a CSP plant but in this case by means of an exergy analysis. They found that the use of an ACC is not an efficient solution from an exergetic point of view for the operation at low exit turbine pressures although they are more competitive at higher pressures.

Hybrid cooling (HC) systems are presented as a potential solution in CSP plants to cope with the disadvantages of each conventional cooling method. They can reduce the water consumption by up to an 80% [9] compared to wet-cooled CSP plants and enhance the performance in warm weather compared to dry-cooled CSP plants [13]. Several studies of HC integrated into thermal power plants can be found in the literature. Most of them are based on modelling and simulation and aim for the evaluation of the performance of the thermal power plant with the HC system in terms of power generation, water consumption reduction and costs. He et al. [14] developed a 1-D model to predict the annual performance and water consumption of three different cooling systems integrated into a geothermal power plant: a natural draft Dry Cooling Tower, a natural draft WCT and a HC system. The simulations were performed taking the weather data of Birdsville, Australia. From the results, it was found that 70% of water can be saved using the HC system in comparison with the WCT for every MW of heat rejection. In the case of Zhai and Rubin [15], the authors carried out the assessment of the performance, water consumption and costs for a HC system integrated into a coal or a natural-gas-fired power plant with and without carbon capture and storage. The HC system was comprised of a wet-cooled condenser and an ACC connected in parallel. The cost model considered the total annualized cost and total levelized cost of electricity. From these results, the authors found reductions of roughly 91% in the water use for the HC system, but an increase of 3-5% of the Levelized Cost of Electricity was observed. The paper concluded that the overall costs would be minimized if the wet cooling system of the HC operated at a 30% of the total cooling load during hot periods. Hu et al. [16] developed a model for a 660 MW steam power plant that integrates a HC system consisting of ACC in series with a WCT. They investigated the heat transfer phenomena and the water and power consumption for three operation modes: only-dry, only-wet and HC modes, with respect to the change in the ambient temperature and relative humidity. It was found that at high ambient temperatures and low relative humidity no benefits were observed for the HC mode since the system operated as an only-wet cooling system. However, at an ambient temperature of 0 ºC, the results were very favorable for the HC operation mode, with a 46.47% less water consumption in comparison to only-wet and a 45.84% less power fan consumption in comparison to only-dry operation mode. Dehaghani et al. [17] developed computational models to predict the water saving of a thermal power plant located in Iran in the case that the current WCT was modified by the use of a HC system (parallel wet and dry cooling system). The results were very promising

showing a 9.4% lower water consumption after the modifications and 64.6% less fan power consumption if a high-precision air flow regulation method was used (fans with variable frequency drives). Tang et al [18] evaluated the performance of a steam power plant with a HC system, consisting in an ACC in parallel with a WCT, at different operating conditions (ambient temperature, relative humidity, heat load, etc). They concluded that the condensation through the ACC was the best option at the following combinations of ambient temperature and thermal load: 16 °C/300 MW, 24 °C/225 MW and 31°C/150 MW. At higher ambient temperatures, the steam condensation should be prioritized through the WCT. On the other hand, the authors of the present paper [19] carried out the theoretical assessment of the best configurations of a HC system integrated into a CSP plant in terms of power generation and water reduction. For this approach, a model of the power block of a CSP plant (Andasol-1 type) which integrates a HC system was implemented in Thermoflex software. The simulation of different configurations of the HC system (composed of an ACHE and a WCT) was carried out: series, parallel, series-parallel and parallel-series and for each one the water consumption and the net power generation were determined. It was found that the most favorable configuration in terms of water saving was series-parallel, resulting in 50% of water consumption reduction when compared to the only-wet cooling option. For this configuration, a 2.5% higher power generation resulted compared to only-dry cooling option. Other authors have investigated hybrid cooling towers (HCT), in which the dry and wet cooling systems are integrated into the same tower. Rezaei et al. [20] developed a model of a HCT able to operate in parallel or series configurations. The HCT included dry and wet sections, being the dry section composed of several compact air-cooled exchangers. Finally, Wei et al. [21] investigated the effect of ambient conditions over the performance of a natural draft HCT and compared it with a natural draft dry cooling tower. It was found that the operation of this hybrid system was more flexible than the natural draft dry cooling tower under variable environmental conditions.

Regarding experimental studies, there are limited research works on HC systems tested in real environment. The existing ones are based on experiments at lab-scale [22,23]. In one of these studies [23], promising results were found when the HC system was selected instead of a conventional wet cooling system, resulting in a 35% less water consumption. These results further demonstrate the need for experiments at pilot-scale in order to provide reliable data for industry. In addition, the urgent need to find the best operational strategies in HC systems that reduce the water requirements in CSP plants is crucial. From the theoretical works presented above, only the one presented by the authors of this paper [19] has considered the integration of a HC system into a CSP plant. This paper complements the previous theoretical study by an exhaustive experimental analysis of a pilot scale HC system installed at the Plataforma Solar de Almería (PSA), in Tabernas (Almería), Spain. This system was manufactured and then installed at PSA

under the framework of an EU H2020 project on Water Saving for Concentrated Solar Power (WASCOP). The pilot HC system consists of an ACHE and a WCT, both sharing a surface condenser that is coupled with a steam generator driven by a solar field. The steam generator generates low-pressure steam (pressure between 82 and 200 mbar) with similar conditions to those obtained in the exhaust steam from the power block of a CSP plant. The HC pilot plant is flexible and allows the HC operation in different configurations like series, parallel, only-wet and only-dry. From the results obtained from the experimental assessment[1], the optimal configurations of the HC system in terms of water and electricity consumption under a wide range of operating (change in the thermal load) and environmental conditions (change in the ambient temperature) has been obtained.

2. Description of the test facility

The HC pilot plant is located at PSA, which is the largest concentrating solar technology research, development and test center in Europe and is a division of the Centro de Investigaciones Energéticas, Medioambientales y Tecnológicas (CIEMAT). PSA is located in Tabernas (Latitude 31.10 N and Longitude 2.36 W) at the South of Spain. A Typical Meteorological Year of Tabernas has been obtained using Meteornom software and the resulting monthly ambient temperature throughout a year is shown in Figure 1.

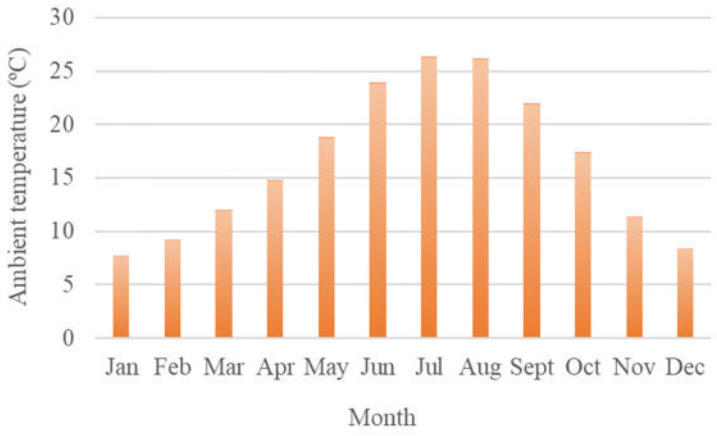

Figure 1. Average monthly data of ambient temperature at PSA-CIEMAT

The HC pilot plant is composed of a WCT and an ACHE that can be tested separately (only-wet, only-dry) or in series/parallel configurations. Fig. 2 shows the simplified schematic diagram of this pilot plant that consists of three main circuits: heating, exchange and cooling.

[1] Based on experiments carried out at PSA-CIEMAT

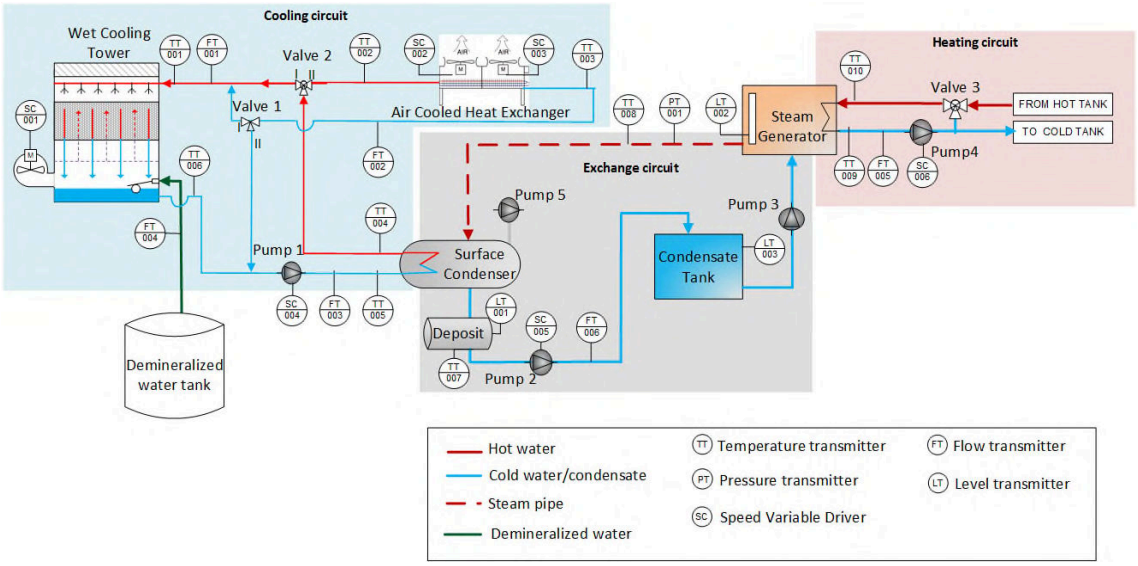

Fig. 2. Schematic diagram of the HC pilot plant at PSA-CIEMAT

2.1. The heating circuit

In the heating circuit, hot water flows inside the tube bundles of a steam generator (see Fig. 2 and Fig. 3 (b)) water, coming from a condensate tank, flows inside the shell of this steam generator. Heat is then transferred from the tubes to the shell and subsequently steam is generated. Hot water is provided from a storage system, which is connected to a 300 kW_{th} flat-plate solar field (see Fig. 3 (a)) by a heat exchanger through which the thermal energy is transferred. For the sake of brevity, no further details about the solar field are given but further information can be found in Chorak et. al [24]. The water flow rate inside the tube bundles of the steam generator (FT-005) is controlled using a Proportional, Integral and Derivative (PID) controller that uses the input to the variable frequency drive of Pump 4 (SC-006 in Fig. 2) as a control signal. On the other hand, the hot water inlet temperature (TT-010) is controlled at the desired value by the aperture of Valve 3. A PID controller acts over the aperture of this valve in order to mix the hot water from the storage system with the colder water coming from the steam generator. By controlling hot water flow rate and inlet temperature in the steam generator, different steam flow rates can be evaluated in the pilot plant. Therefore, it allows the operation of the HC system at different thermal loads, simulating thus its integration into a real CSP plant that usually is under partial load conditions due to the solar radiation variability.

(a) (b)

Fig. 3. HC pilot plant at PSA-CIEMAT: a) flat-plate collectors of the heating circuit, b) steam generator: hot water inlet (1) and outlet (2).

2.2. The exchange circuit

In the exchange circuit, a vacuum system (Pump 5 in Fig. 2) connected to a surface condenser allows choosing the desired vacuum pressure in the circuit by a Programmable Logic Controller (PLC) (in the range 82-200 mbar). The steam generated flows to the surface condenser (see Fig. 2 and Fig. 4) where it is condensed while releasing the condensation heat to the cooling water circulating inside the tube bundle, which is in turn heated. The condensate from the surface condenser flows by gravity to a small deposit and it is then pumped to a condensate tank. The variable frequency drive of Pump 2 (SC-005 in Fig. 2) maintains the condensate level (LT-001 in Fig. 2) inside such deposit. Finally, water inside the condensate tank is pumped to the steam generator through Pump 3, closing the exchange circuit. This pump is turned on/off to maintain the level of liquid inside the steam generator (LT-002 in Fig. 2) at the desired value. Technical data of the steam generator and the surface condenser can be found in Table 1.

(a) (b)

Fig. 4.HC pilot plant at PSA-CIEMAT, exchange circuit: (a) steam generator (1) and surface condenser (2), (b) surface condenser (1), condensate tank (2) and small deposit under the surface condenser (3).

2.3. The cooling circuit

The cooling circuit is composed of an ACHE and a WCT (see Fig. 2 and Fig. 5). Cooling water coming from both towers is pumped to the tube bundle of the surface condenser where it is heated by the heat transferred by condensation of the steam generated by the steam generator. Then, the heated cooling water flows back to the hybrid cooler to repeat the cooling process. The aperture of Valves 1 and 2 are modified to choose the desired configuration (see Table 2 and Fig. 2): only-dry, only-wet, series or parallel. In addition, a split ratio (defined as the wet fraction) can be selected in parallel configuration. The water flow rate in the tube bundle of the surface condenser (FT-003 in Fig. 2) is controlled using a PID controller that uses the variable frequency drive of Pump 1 (SC-004 Fig. 2) as control signal to maintain the nominal operating conditions despite the different head losses existing in each configuration. On the other hand, the variable frequency drives of the fans in both cooling towers (SC-001, SC-002 and SC-003 in Fig. 2) are used as control variables to maintain the inlet temperature to the surface condenser (TT-005 Fig. 2) at the desired value. Although most of the water in the cooling circuit recirculates, a small percentage of water evaporates in the WCT and must be replaced. A float valve installed in the WTC basin allows filling it with make-up water when the water level goes down. The make-up water consumed by the WCT is measured by a flow meter located at the inlet of this cooling tower (FT-004). Technical data of the cooling systems can be found in Table 1.

Fig. 5. Cooling circuit in the HC pilot plant at PSA-CIEMAT. WCT (1) and ACHE (2)

Table 1
Technical data of the equipment in the cooling and exchange circuits.

Steam generator	
Thermal power @42ºC	80 kW_{th}
Tube side	Hot water
Shell side	Cold water/Steam

Surface condenser		
	Thermal power @42ºC	80 kW_{th}
	Tube side	Water
	Shell side	Steam
WCT		
	Thermal power	204 kW_{th}
	Evaporation	0.28 m3/h
ACHE		
	Capacity	204 kW_{th}
	Exchange surface	617.58 m^2
	Power consumption	5.67 kW_e

Table 2
Configurations in the cooling circuit (see valve positions I and II in Fig. 2)

	Valve positions	
Configuration	Valve 1	Valve 2
Only-dry	II	II
Only-wet	-	I
Series	I	II
Parallel split ratio	II	Between I and II to achieve the desired split ratio

3. Methodology

3.1. Test campaign

The test campaign was designed to evaluate the different configurations of the HC system as a function of the ambient and operating conditions. Table 3 shows the range of variation for all of the variables. A total of 54 experiments were conducted in the year 2020 and 2021 and they were designed as follows:

- Three ambient temperature ranges were selected in order to cover the different seasons of the year in the location of Tabernas (Almería). This way, ambient temperature between 10 and 15 ºC would represent the operation of the HC system in winter, ambient temperature between 18 and 23 ºC would represent the operation of the HC system in spring and autumn and ambient temperature between 25 and 30 ºC would represent the operation of the HC system in summer (see Figure 1).
- For each ambient temperature range, three thermal loads of the surface condenser were tested; a partial load of 60%, which corresponds to a thermal power between 120-125 kW_{th}; a partial load of 80%, which corresponds to a thermal power between 170- 175 kW_{th} and nominal conditions (i.e., thermal load of 100%) that corresponds to a thermal load between 200-225 kW_{th}.
- For each ambient temperature range and for the three thermal loads, configurations only-dry (DC), only-wet (WC), series (SS) and parallel were tested. In the case of DC, WC

and SS, the maximum cooling flow rate (24 m^3/h) circulates through both cooling towers. In the case of parallel configurations, three split ratios were tested by the use of Valves 1 and 2 of cooling circuit (see Table 2 and Fig. 2): 25%, 50% and 75% for configurations P25, P50 and P75, respectively. In the case of P25, FT-001 is 6 m^3/h and FT-002 is 18 m^3/h; in the case of P50, FT-001 and FT-002 is 12 m^3/h and in the case of P75, FT-001 is 18 m^3/h and FT-002 is 6 m^3/h. The set point of cooling flow rate was established in the variable frequency drive of pump 1 (SC-004 in Fig. 2).

- In all tests, the temperature of the steam produced by the steam generator (TT-008 in Fig. 2), which would represent the exhaust steam from a turbine in a CSP plant, was maintained at 45 ºC, which is the typical condensation temperature in a CSP plant located at the South of Europe. It was controlled by establishing a set point of vacuum pressure in the PLC of the vacuum system (Pump 5 in Fig. 2).

- In all tests, the hot water flow rate flowing inside the tube bundle of the steam generator (FT 005 in Fig. 2) was kept at 9.75 L/s. On the other hand, the hot water inlet temperature in the steam generator (TT-010) varied between 68 ºC and 76.5 ºC to assure the thermal loads above-mentioned.

- Finally, the temperature at the inlet of the surface condenser (TT-005 in Fig. 2) was established in all cases at 33 ºC (i.e., the design temperature of this equipment). It was established by the control of the variable frequency drives of both cooling towers (SC-001, SC-002 and SC-003 in Fig. 2). In the case of series configuration, as the cooling water is cooled firstly through the ACHE and then through the WCT, the temperatures at the outlet of the ACHE (TT-003 in Fig. 2) and WCT (TT-006 in Fig. 2) were maintained at 36 ºC and 33 ºC, respectively.

Table 3
Range of variation of the ambient and operating variables

Variable	Range of operation
Ambient temperature, T_{amb}	(10-30) ºC
Thermal load, TL	(60-100) %
Cooling water flow rate through the ACHE, FT-002	(6-24) m^3/h
Cooling water flow rate through the WCT, FT-001	(6-24) m^3/h
Hot water inlet temperature in the steam generator, TE-WAS-010	(68-73.5) ºC
Variable frequency drives (VFD) of the ACHE, SC-002 and SC003	(11-98)%
Variable frequency drive (VFD) of the WCT,	(21-100)%

It is important to ensure steady state conditions during the operation of the HC, especially in the steam flow rate generated by the steam generator and in the make-up water consumed by the WCT (FT-004 in Fig. 2). In the case of the generated steam, the level of the steam generator (LT-002 in Fig. 2) was maintained to be stable as possible around 330 mm in order to assure that the tube bundles were completely flooded. The water circulation from the surface condenser to the condensate tank was also kept as steady as possible. For that purpose, the level in the small deposit at the outlet of the surface condenser (LT-001 in Fig. 2) was maintained around 200 mm.

The data was logged every second and the average value of each variable was determined in a steady stage period of between 15-20 minutes. An error analysis was performed considering the measurement uncertainties of all the instruments. In the case of the indirect parameters an uncertainty propagation analysis was carried out in order to quantify the goodness of the results. For this purpose, a tool from the Engineering Equation Solver software described in NIST Technical Note 1297 was used [25]. The measurement uncertainties of all measured variables are shown in Table 4.

Table 4
Measurement uncertainty of the direct variables

Parameter	Measurement uncertainty
Electricity consumed by the WCT, ACHE and pump 1	1%
Make-up water consumed by the WCT	± 0.5% of F.S[a] + 2.5% o.r[b]
Condensate mass flow rate	± 0.2% o.r[b]
Saturated steam pressure	± 0.3% o.r[b] + 0.8% of URL[a]
Temperatures	0.3+0.005·T[c]

[a]F.S = full scale. It is 10 for FT-WAS-004 and 1.1 bar for PT-001

[b]o.r = of reading

[c]is the value of the temperature in ºC

3.2. Assessment of the hybrid configurations

The HC configurations were evaluated by determining the improvements achieved in terms of electricity consumption reduction, in comparison to only-dry operation mode (i.e. (ec_{DC}-ec_{HC})/ec_{DC}) and in terms of water consumption reduction, in comparison with only-wet operation mode (i.e. (wc_{WC}-wc_{HC})/wc_{WC}). ec_{HC} and ec_{DC} are the electricity consumptions of the hybrid and DC configurations, respectively, and wc_{HC} and wc_{WC} are the water consumptions of the hybrid and WC configurations, respectively. The results obtained at different thermal loads and ambient temperatures are shown and explained in section 4.

The following sections describe the calculations of the electricity and water consumptions.

3.1.1. Electricity consumption

The electricity consumption (ec) is measured with an electrical energy meter (CEM-C21) installed in the electrical distribution panel of the facility that provides the instantaneous power consumption of the Pump 1 and of WCT and ACHE fans. This consumption depends on the percentage applied to the corresponding VFD, as can be observed in Fig. 6.

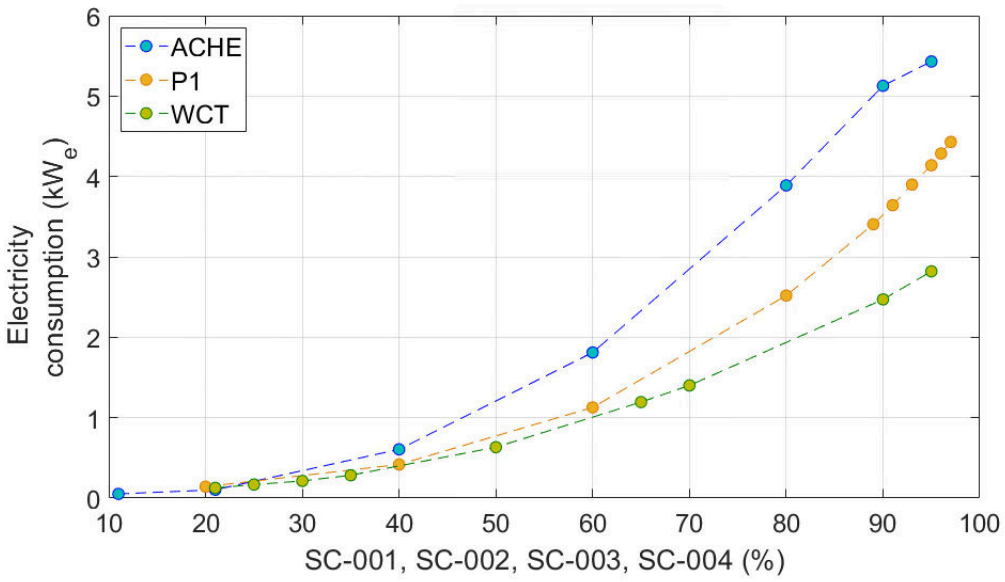

Fig. 6. Electricity consumption measurements at different percentages applied to the VFDs.

The total electricity consumption measured is the sum of each one of the contributions. It is important to highlight that the operating point of Pump 1 in the experimental campaign described in this paper corresponds to values in the VFD, SC-004, between 91% and 97%. In the case of the ACHE operation, the values in the experimental campaign analyzed in this paper cover the whole range of SC-002 and SC-003 depicted in Fig. 6, while in the case of the WCT operation, the maximum percentage required in SC-001 has been 40%.

3.1.2. Water consumption

As already mentioned, wc is measured by a flow meter located at the inlet of the make-up water pipe (FT-004 in Fig. 2). As it is evaluated when steady-state conditions are reached, the make-up flow can be considered to correspond to the water evaporated in the WCT.

3.3. Efficiency calculation and selection of optimal configurations

Two efficiency indexes that determine the specific electricity energy consumption (SEC) and the specific water consumption (SWC) are proposed to decide which is the optimal configuration according to the ambient and operating conditions. There must be a trade-off between the water and the electricity consumption, considering also the relation of these values with the thermal power. In other words, the optimal configurations will be the ones that allow reducing as much as possible the water and electricity consumptions per kW_{th} used to condensate the available steam. The calculation of these indexes is as follows:

$$SEC\left(\frac{kW_e}{kW_{th}}\right) = \frac{ec}{TP}\ , \qquad (1)$$

$$SWC\left(\frac{L/h}{kW_{th}}\right) = \frac{wc}{TP}\ , \qquad (2)$$

where ec is the electricity consumption measured in kW_e, wc is the water consumption in L/h and TP is the thermal power of the surface condenser measured in kW_{th}. It is defined as the heat transfer rate by condensation of the steam generated and can be determined by Eq.**Error! Reference source not found.**:

$$TP = \dot{m}_s\lambda_{cond} + \dot{m}_c(h_{l,sat} - h_c), \qquad (3)$$

where $\dot{m}_s$ is the steam mass flow rate generated by the steam generator, λ_{cond} is the latent heat of condensation at the pressure measured in PT-001 (see Fig. 2), $\dot{m}_c$ is the condensate mass flow rate at the outlet of the surface condenser, $h_{l,sat}$ is the specific enthalpy of saturated liquid in the surface condenser at pressure PT-001 and h_c is the specific enthalpy of the subcooled condensate leaving the surface condenser, at the temperature TT-007 (see Fig. 2) and pressure PT-001.

Notice that, as the evaluation of the HC is performed at steady state conditions, the steam entering the surface condenser is completely condensed, so it can be assumed that $\dot{m}_s = \dot{m}_c$. In addition, the VFD of Pump 2 is regulated to maintain LT-001 at a steady-state value, so the mass flow rate at the outlet of the surface condenser ($\dot{m}_c$) is that measured in FT-006 (see Fig. 2).

The optimal configurations are obtained by a cost function, J_{ijk}, which is evaluated for each configuration, *i*, thermal load, *j*, and ambient temperature, *k*, being *i*={WC,P75,P50,P25,SS,DC}, *j*={TL-60,TL-80,TL-100} and *k*={(10-15), (18-23), (25-30)} ºC:

$$J_{ijk} = \alpha_1 \cdot \frac{SEC_{ijk} - SEC_{jk}^{min}}{SEC_{jk}^{max} - SEC_{jk}^{min}} + \alpha_2 \cdot \frac{SWC_{ijk} - SWC_{jk}^{min}}{SWC_{jk}^{max} - SWC_{jk}^{min}}, \qquad (4)$$

$$SEC_{jk}^{min} = \min\{SEC_{ijk}\} \qquad \forall\, i = \{WC, P75, P50, P25, SS, DC\}, \tag{5}$$

$$SEC_{jk}^{max} = \max\{SEC_{ijk}\} \qquad \forall\, i = \{WC, P75, P50, P25, SS, DC\}, \tag{6}$$

where SEC and SWC are normalized to bring all values into the range [0,1] and α_1 and α_2 are weighting factors to tune the importance of each term in relation to the other. In this case, the values established for these factors are: α_1=1 and α_2=1.2, because the priority is to reduce the water consumption. The optimal value for each load and ambient temperature range, θ_{jk}, corresponds to that configuration that gives the minimum value of J:

$$\theta_{jk} = \min_i\{J_{ijk}\} \qquad \forall\, i = \{WC, P75, P50, P25, SS, DC\}. \tag{7}$$

4. Results

4.1 Variation of the electricity consumption

This section shows the variation of the electricity consumption and of the temperatures in the cooling circuit (i.e., the inlet and outlet temperatures from the ACHE and WCT) with the TL and with the ambient temperature for the different HC configurations (see Fig. 7 and Figure *8*). TL-100 corresponds to the operation at thermal load 100%, TL-80 to the operation at thermal load 80% and TL-60 to the operation at thermal load 60%. In addition, this section shows the percentages of ec reduction of the HC configurations in comparison to configuration only-dry (the one with the highest electricity consumption) for the different TL and ambient temperature ranges (see Table 5). The errors obtained from the uncertainty propagation analysis are also shown in this table together with the percentage results.

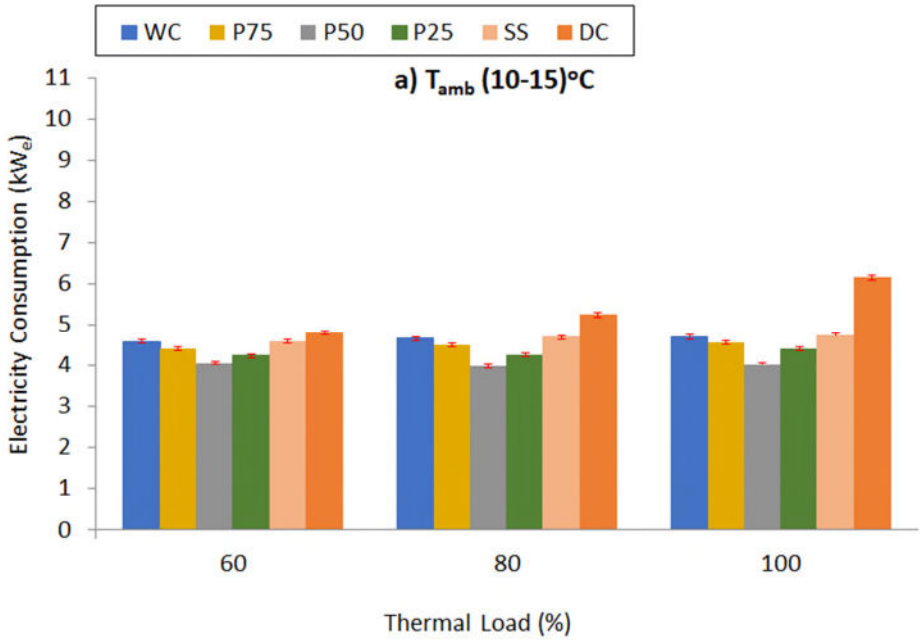
WC
P75
P50
P25
SS
DC
a) T_{amb} (10-15)°C
Electricity Consumption (kW_e)
0
1
2
3
4
5
6
7
8
9
10
11
60
80
100
Thermal Load (%)

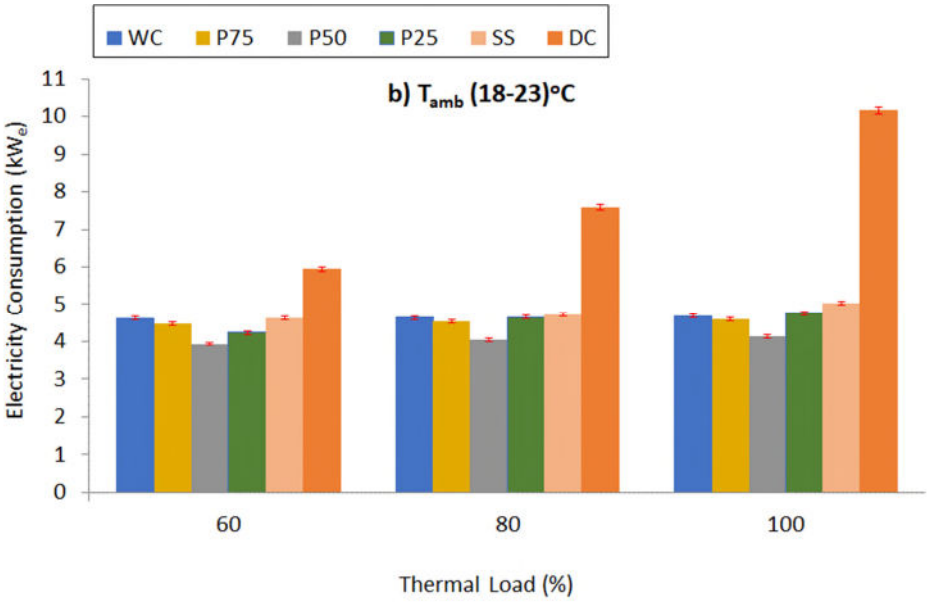
WC
P75
P50
P25
SS
DC
b) T_{amb} (18-23)°C
Electricity Consumption (kW_e)
0
1
2
3
4
5
6
7
8
9
10
11
60
80
100
Thermal Load (%)

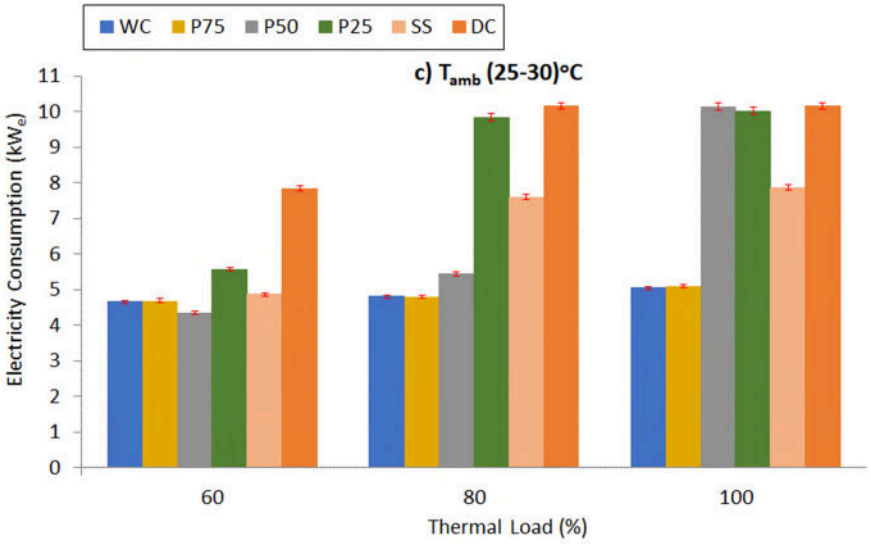

Figure 7. Effect of the thermal load on the electricity consumption for a) T_{amb} (10-15) ºC; b) (18-23) ºC and c) (25-30) ºC. All the errors are represented as error bars

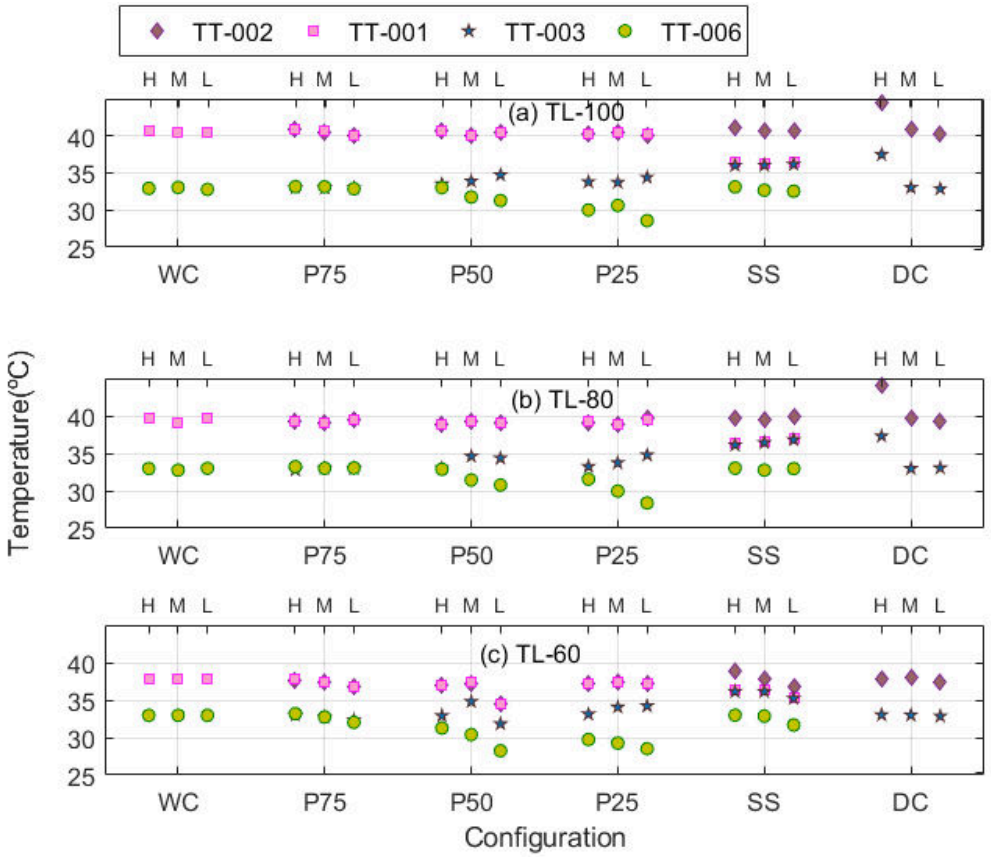

Figure 8. Temperatures in the cooling circuit at different ambient temperature ranges (H: (25-30) ºC, M: (18-23) ºC, L: (13-15) ºC) at a TL (a) 100%, (b) 80% and (c) 60%. The maximum error of the temperature measurements is 0.5 ºC (see Table 1).

As observed in Fig. 7, the value of ec increased in all configurations with the thermal load and with the ambient temperature. The increase with the thermal load is explained by the rise in the cooling water temperatures at the inlet of the WCT and ACHE (TT-001 and TT-002, respectively)

when the TP in the surface condenser increases, as can be seen in Figure 8. Such temperature rise leads to a higher percentage required in SC-001, SC-002 and SC-003 to achieve the desired temperature at the inlet of the surface condenser (33 ºC). Likewise, higher percentages in SC-001, SC-002 and SC-003 are directly related with a higher electricity consumption of the cooling system, as indicated in Fig. 6. On the other hand, the higher the ambient temperature the higher the percentage needed in the VFD of both cooling towers to achieve the cooling requirements, which leads to a rise in the ec, as seen in Fig. 6. This ec increase is especially significant in the case of the ACHE (configuration DC), as seen in Fig. 7, since in this case the ec increases at a higher rate the higher the percentage used in SC-002 and SC-003 is. For the rest of configurations, it can be seen that at low and medium ambient temperatures, there are no significant differences between them in terms of ec, for the different thermal loads. It can be seen that WC, SS, P75 and P25 have similar ec, and configuration P50 was the one with the lowest electricity consumptions. It is important to highlight that, although a lower ec for configuration WC is expected compared with the HC configurations, the head losses in the cooling circuit for this configuration are higher than for the others, which led to a higher electricity consumed by Pump 1. At high ambient temperatures, the differences in ec between configurations became more significant, especially at higher thermal loads. At TL-80, the configurations that showed the highest ec were P25 and SS and at TL-100, P50 and SS.

The results shown in Table 5 can help selecting the most suitable configurations in terms of ec reduction compared to the conventional only-dry cooling system. As it can be seen, the ec reduction of configurations P50, P75, P25, WC and SS with respect the configuration only-dry was higher the higher the thermal load and ambient temperature were. This is a reasonable result given the reasons mentioned before regarding the significant effect of both variables (TL and ambient temperature) in the ec of the ACHE. At low ambient temperatures (i.e., between 10 and 15 ºC) and the lowest TL (TL-60), the percentage of reduction in the ec with respect to the operation with configuration only-dry was not very significant, being the highest one 11.7% for configuration P25. When the TL was increased up to 80%, the percentage of ec reduction compared to only-dry became more significant for some configurations, being P50 the one that showed the higher ec reduction (24.0%), followed by P25 that obtained a percentage of ec reduction of 18.9%. At nominal conditions (TL-100), the HC operation allowed an important ec reduction compared to the conventional only-dry operation and the same configurations as before (P50 or P25) achieved higher improvements in terms of ec (the percentages of reduction were 34.7% and 28.6%, respectively). At medium ambient temperatures (i.e., between 18 and 23 ºC), the percentages of ec reduction increased with respect to the operation at low ambient temperatures, being more pronounced at higher TLs. In the case of TL-60, the recommended configuration in terms of ec saving would be P50, since it showed the highest ec reduction

(34.0%). At TL-80, apart from P50 (whose percentage of ec reduction compared with DC was 46.7%), P75 also gave good results (40.0% of ec reduction), so these two HC configurations could be suitable in case ec is prioritized. At nominal load, the same HC configurations are recommended in terms of ec reduction. Finally, at high ambient temperatures (i.e. between 25 and 30 ºC), the percentages of ec reduction in comparison with the only-dry configuration were the highest ones, achieving values close to 50%. Among the tests performed at the lowest TL, it was found that the operation with configurations P50, P75 and WC is recommended when a significant ec reduction is required compared with the conventional only-dry configuration. The percentages of reduction obtained were 44.4% for P50, 40.1% for P75 and 40.6% for WC.

Table 5
Percentages of electricity consumption reduction of the HC configurations with the associated errors in comparison to configuration only-dry for the different thermal loads and ambient temperature ranges

		Ambient temperature ranges		
Configuration	Thermal Load	(10-15) ºC	(18-23) ºC	(25-30) ºC
WC	TL-60	(4.6±1.3)%	(22.4±1.1)%	(40.6±0.8)%
	TL-80	(11.2±1.3)%	(38.8±0.9)%	(52.7±0.7)%
	TL-100	(23.7±1.1)%	(53.8±0.7)%	(49.7±0.7)%
P75	TL-60	(8.1±1.2)%	(24.7±1.1)%	(40.1±0.8)%
	TL-80	(14.5±1.2)%	(40.0±0.8)%	(52.7±0.7)%
	TL-100	(25.8±1.1)%	(54.6±0.6)%	(49.7±0.7)%
P50	TL-60	(22.7±1.2)%	(34.0±0.9)%	(44.4±0.8)%
	TL-80	(24.0±1.1)%	(46.7±0.7)%	(46.4±0.8)%
	TL-100	(34.7±0.9)%	(59.4±0.6)%	(0.0±1.4)%
P25	TL-60	(15.4±1.2)%	(28.7±1.0)%	(28.8±1.0)%
	TL-80	(18.9±1.1)%	(38.6±0.9)%	(3.1±1.4)%
	TL-100	(28.6±0.9)%	(53.2±0.7)%	(1.4±1.4)%
SS	TL-60	(4.4±1.3)%	(22.2±1.1)%	(37.9±0.9)%
	TL-80	(10.7±1.3)%	(37.6±0.9)%	(25.2±1.1)%
	TL-100	(23.1±1.1)%	(50.6±0.7)%	(22.4±1.1)%

4.2 Variation of the water consumption

This Section shows the variation of the water consumption of the HC at different TL and ambient temperature (see Figure 9). In addition, it shows the percentages of wc reduction of the HC configurations in comparison to configuration only-wet, which can be found in Table 6.

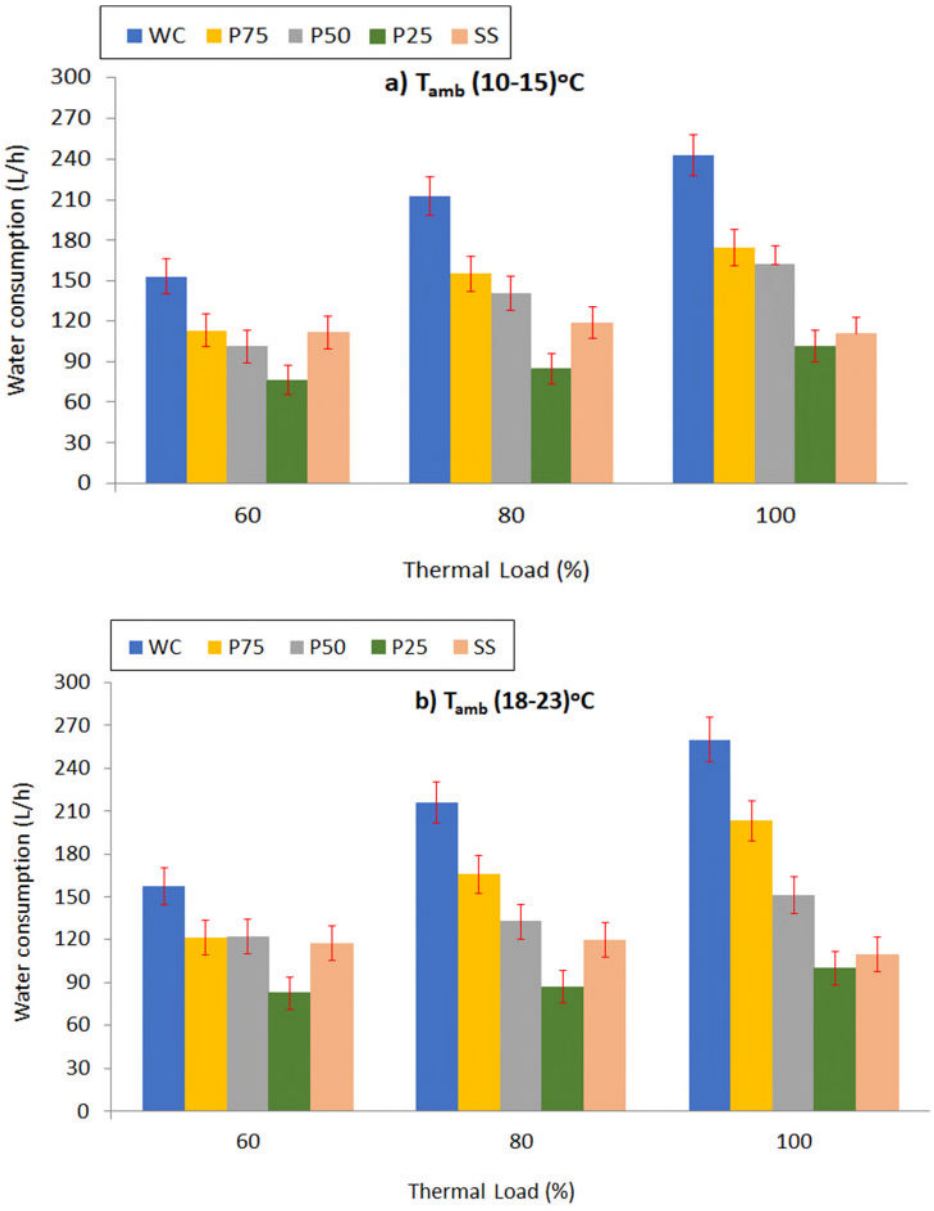

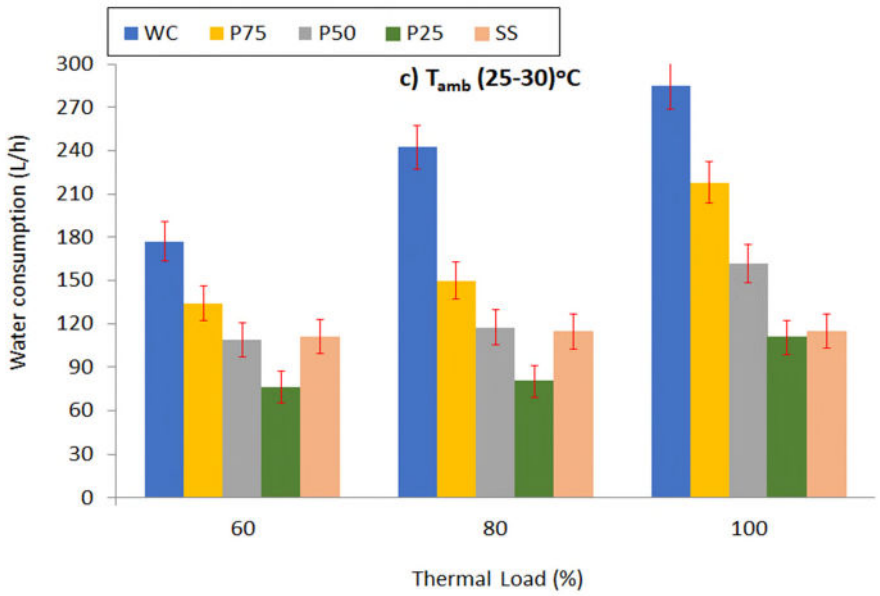

Figure 9. Effect of the thermal load on the water consumption for a) T_{amb} (10-15) ºC; b) (18-23) ºC and c) (25-30) ºC. All the errors are represented as error bars

As observed in Figure 9, w*c* increased in all configurations with the thermal load, except in the case of configuration SS. This increase is due to the rise in the cooling water temperature at the inlet of the WCT with the thermal load (see Figure 8). An increase in this cooling water temperature leads to a higher energy demand required to reduce the enthalpy of the water through the WCT to reach the desired 33 ºC at the outlet. Then, the air flow rate must increase (by means of the VFD of the fan) in order to cover such energy demand, causing higher losses by evaporation and consequently higher water consumptions. In series configuration, w*c* presented similar values at different TLs because the cooling water temperature at the inlet of the WCT (TT-001 in Figure 8) was maintained at 36 ºC. This makes the VFD of the fan work at similar operating conditions, being the air flow rate then similar and therefore the losses by evaporation.

Regarding the behaviour of the w*c* with respect to the ambient temperature, it is expected that the water consumption in the WCT increases with increasing ambient temperature because the energy demand required to reduce the enthalpy of the water through the tower (and reach 33 ºC at the outlet) depends on the air enthalpy difference between the outlet and the inlet. Since the air inlet enthalpy increases with the ambient temperature, the air flow rate must increase (by means of the VFD of the fan) in order to cover the energy demand, causing higher losses by evaporation (i.e., higher water consumptions). As seen in Figure 9, this increase was observed in the case of configurations WC and P75. However, in the case of P50 and P25 configurations, the tendency was opposite to the previous cases and the w*c* decreased with the ambient temperature. This fact is directly related to the cooling capacity of the WCT. When the WCT is operating with medium-low cooling flow rates (12 m^3/h in the case of P50 and 6 m^3/h in the case of P25) and the ambient

temperature and/or the water inlet enthalpy are low (i.e. partial loads), the temperature at the outlet of the WCT (TT-006 in Figure 8) is under 33 ºC because the minimum fan percentage (21%) is achieved. Therefore, the air mass flow in these cases is higher than needed in order to achieve the required operating conditions and the losses by evaporation are higher than expected. To understand this fact better, configuration P50 at TL-100 is taken as an example. At low ambient temperature, the VFD of the WCT was at the minimum value, and the outlet temperature of the WCT was lower than required, 30 ºC. Then, it canseen in Figure 8 that the temperature difference between the inlet (TT-001) and the outlet of the WCT (TT-006) was higher at low ambient temperatures than at high ambient temperatures, which is directly related to the water consumption as explained previously.

In the case of SS configuration, as already mentioned, the water inlet temperature to the WCT is always maintained at 36 ºC (TT-001 in Figure 8), and a similar water consumption can be observed for the three ambient temperature ranges. This is caused because the temperature difference between the inlet and outlet temperatures in the WCT was low (only 3 ºC), which led to a low required heat transfer to achieve this temperature difference through water evaporation.

The comparison between configurations was carried out by evaluating the water consumption reduction in the case of using a HC configuration instead of a only-wet configuration, which is the configuration with the highest wc. The values obtained together with the resulting errors from the uncertainty propagation analysis can be found in Table 6.

Table 6
Percentages of water consumption reduction of the HC configurations with the associated errors in comparison to configuration only-wet for the different thermal loads and ambient temperature ranges.

		Ambient temperature ranges		
Configuration	Thermal Load	(10-15) ºC	(18-23) ºC	(25-30) ºC
P75	TL-60	(26.2±9.9)%	(23.2±10.0)%	(24.2±9.1)%
	TL-80	(26.9±7.9)%	(23.0±8.02)%	(38.1±6.5)%
	TL-100	(27.9±7.1)%	(21.8±7.2)%	(23.6±6.7)%
P50	TL-60	(33.9±9.4)%	(22.8±10.0)%	(38.7±8.1)%
	TL-80	(33.6±7.4)%	(38.6±7.1)%	(51.6±5.8)%
	TL-100	(33.0±6.8)%	(41.6±6.1)%	(43.3±5.6)%
P25	TL-60	(50.2±8.3)%	(47.8±8.3)%	(56.9±7.0)%
	TL-80	(60.4±5.9)%	(59.7±5.9)%	(66.9±5.0)%
	TL-100	(58.2±5.4)%	(61.6±5.0)%	(61.3±4.7)%
	TL-60	(27.2±9.9)%	(25.6±9.8)%	(37.3±8.2)%

SS	TL-80	(44.3±6.8)%	(44.7±6.7)%	(52.8±5.7)%
	TL-100	(54.4±5.6)%	(57.9±5.2)%	(59.7±4.8)%

As expected, the highest wc reduction was obtained from configuration P25 (66.9% at high ambient temperature and TL-80) since this is the configuration with the least use of the WCT, with only 6 m^3/h of water flow rate through the WCT. On the opposite side, P75 was the HC configuration that makes the highest use of the WCT (18 m^3/h of water flow rate) so it achieved the lowest water reduction in comparison to configuration only-wet (24.2% at medium ambient temperature and TL-60).

The water consumption reduction in configuration P25 increased with TL and ambient temperature between 50.2% and 66.9%, a considerable reduction that emphasizes the importance of combining wet and dry cooling to reduce the water consumption along the year and for all thermal loads. In the case of SS configuration, the percentages of water consumption reduction also increased with the ambient temperature and TL but it was more significant at TL-80 and TL-100 (between 44.7% and 59.7%). At low thermal load, TL-60, the percentage of increase was between 25.6% and 37.2%, which was closer to the values obtained with parallel configurations. The percentages of increase with configuration P50 were lower than in the previous cases and did not show a specific tendency with the ambient temperature and the TL because of the WCT cooling capacity limitation in some of the experiments, as explained previously. In the case of configuration P75, the percentages at different TLs and several ambient temperatures varied over a narrow range (between 21.8% and 27.9%), and did not follow a clear tendency because the water consumption in this configuration was closer to the one obtained with configuration only-wet.

4.2. Optimal configurations

Fig. 10 shows the results of SEC and SWC obtained for each one of the configurations, thermal loads and ambient temperature ranges. The maximum error obtained from the uncertainty analysis resulted of 0.0007 kW_e/kW_{th} and 0.11 $L/h \cdot kW_{th}$ for the SEC and SWC, respectively. The optimal configurations obtained are represented in bold type.

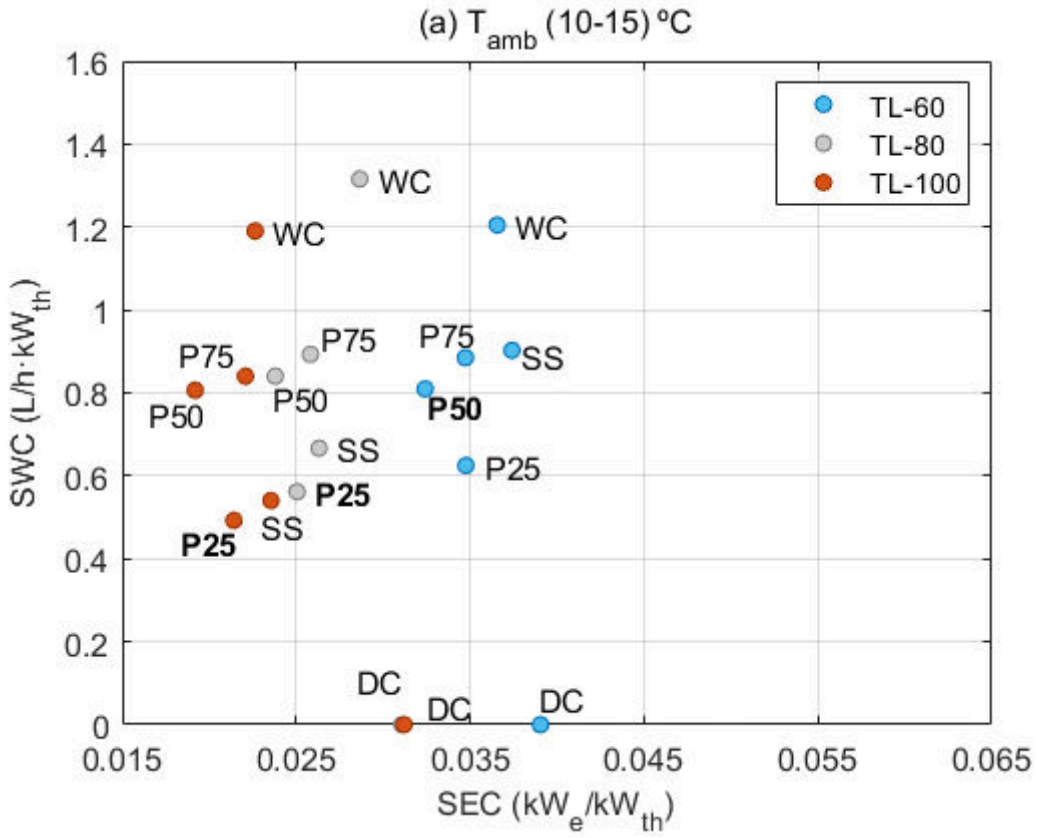
(a) T amb (10-15) ºC
TL-60
TL-80
TL-100
WC
WC
WC
P75
P75
P75
SS
P75
P50
P50
P50
SS
P25
P25
SS
P25
DC
DC
DC
SWC (L/h·kW th)
SEC (kW e/kW th)
1.6
1.4
1.2
1
0.8
0.6
0.4
0.2
0
0.015
0.025
0.035
0.045
0.055
0.065

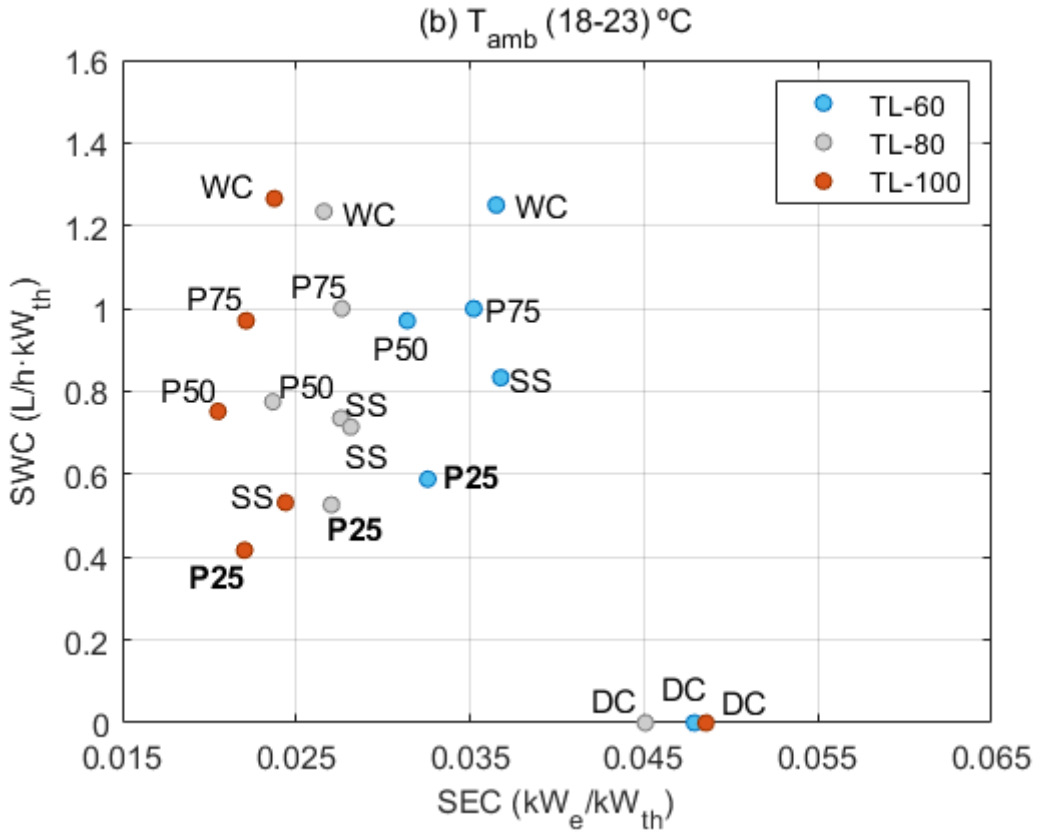
(b) T amb (18-23) ºC
TL-60
TL-80
TL-100
WC
WC
WC
P75
P75
P75
P50
P50
P50
SS
SS
SS
SS
P25
P25
P25
DC
DC
DC
SWC (L/h·kW th)
SEC (kW e/kW th)
1.6
1.4
1.2
1
0.8
0.6
0.4
0.2
0
0.015
0.025
0.035
0.045
0.055
0.065

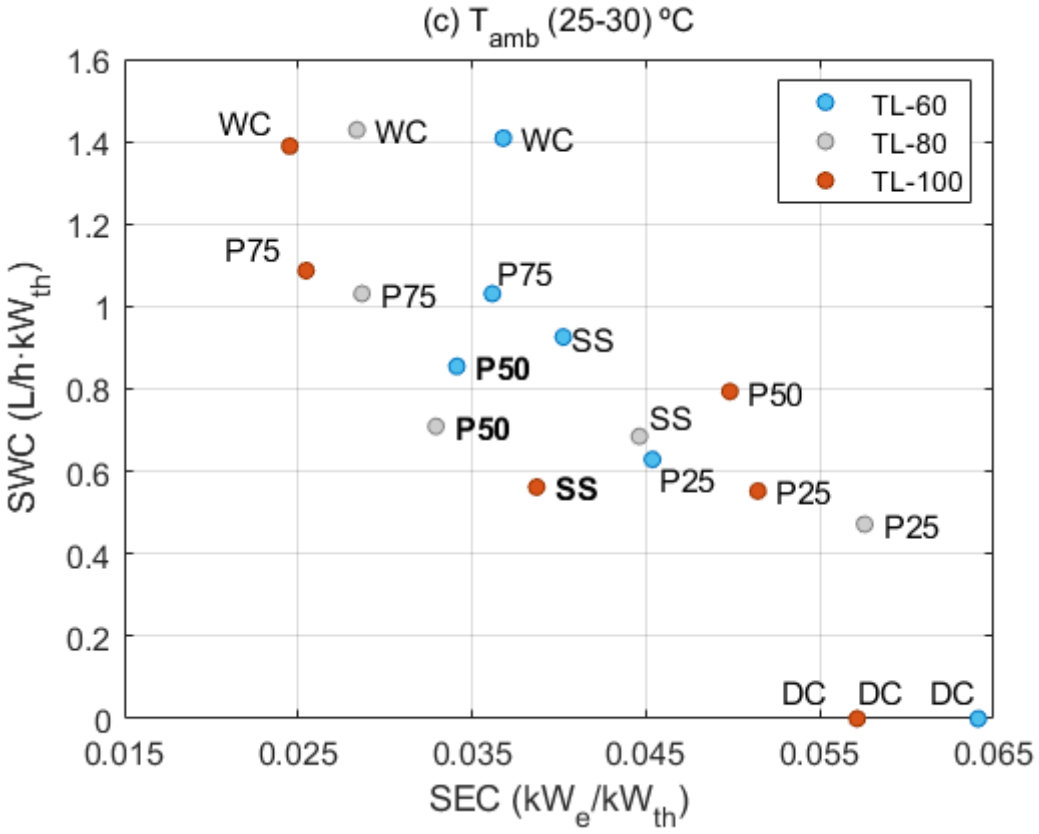

Fig. 10. *SWC* against *SEC* for each configuration, at different thermal loads and at different ambient temperature ranges (a) (10-15) ºC, (b) (18-23) ºC and (c) (25-30) ºC. Optimal configurations are represented in bold type.

At low ambient temperatures (Fig. 10 (a)), the best results were obtained from configuration P25 at TL-60 and TL-80. At this ambient temperature, the electricity consumption in the ACHE is low, so it is recommendable to operate as much as possible with this configuration in order to reduce the water consumption. At TL-100, configuration P50 presented better results than P25, due to the difference of the electricity consumption between these two configurations. Configuration P25 resulted also the best one in the case of medium ambient temperatures (Fig. 10 (b)), but it is also important to highlight that configuration P50 allowed to reduce the SEC even more at the expense of increasing the SWC. It is important to mention that in all ambient temperature ranges, the lowest specific consumptions were obtained operating at TL-100, which means that partial loads penalize the consumption per kW_{th}. In the case of high ambient temperatures (Fig. 10 (c)), the specific consumptions increased, mainly because of the electricity consumption in the ACHE. For this reason, at high ambient temperatures it would be recommendable to reduce the use of the ACHE, being the optimal configurations SS at TL-100 and P50 at TL-80 and TL-60.

5. Conclusions

This study deals with the assessment of the best operating strategies of a HC system in terms of reduction in the water and electricity consumptions in comparison with the conventional only-dry and only-wet cooling systems. An exhaustive experimental campaign has been carried out at a HC pilot plant at PSA-CIEMAT, testing different configurations under a wide range of operating (different thermal loads) and ambient (different ambient temperatures) conditions. The results obtained from this study can help the CSP industry to invest in HC solutions at industrial scale, since it has been proven that there are strategies that allow to reach a trade-off between the water and the electricity consumption depending on the thermal load of the power block and on the ambient temperature. The main conclusions obtained from the experimental evaluation are detailed below:

- The most favorable configuration in terms of reduction in the electricity consumption at all tested conditions is parallel with a split ratio of 50%. For this configuration, a maximum reduction of 59.3% was obtained compared to only-dry configuration, at nominal load (TL-100) and high ambient temperature (25-30 ºC).

- Configuration parallel with a split ratio of 25% has shown the highest reduction in the water consumption when compared with conventional only-wet configuration. A percentage of 66.6% was obtained when the pilot plant operated at a thermal load of 80% and the ambient temperature was between 25 and 30 ºC.

- The assessment of the optimal operating strategies has been done by the evaluation of two efficiency indicators, which consider the relation of the water and electricity consumptions with the thermal power required to condensate the available steam. These efficiency indicators are the $\boldsymbol{SEC}$ and the $\boldsymbol{SWC}$.

- At low ambient temperatures, the optimal strategy at partial loads (TL-80 and TL-100) is the operation with configuration parallel with split ratio of 25%. However, when the load is reduced to TL-60, it is recommended to change the strategy, operating with configuration parallel with split ratio of 50%.

- At medium ambient temperatures, the best strategy is to operate with configuration parallel with a split ratio of 25% at all thermal loads.

- In the case of high ambient temperatures, the most favorable strategy at partial loads (TL-60 and TL-80) is the operation with configuration parallel with a split ratio of 50%.

When the thermal load increases at TL-100, the strategy should be changed to configuration series that provide an optimal trade-off between the water and electricity consumption.

Nomenclature

Symbols

TP	Thermal power, kW_{th}
Ec	Electricity consumption in the cooling circuit, kW_e
ec_{DC}	Electricity consumption in only-dry configuration, kW_e
ec_{HC}	Electricity consumption in a hybrid configuration, kW_e
ec_{WC}	Electricity consumption in only-wet configuration, kW_e
$\boldsymbol{h_c}$	Specific enthalpy of the condensate, kJ/kg
$\boldsymbol{h_{l,sat}}$	Specific enthalpy of the saturated liquid, kJ/kg
$\dot{m}_c$	Condensate mass flow rate (FT-006 in Fig. 2), kg/s
$\dot{m}_s$	Steam mass flow rate between the steam generator and the surface condenser, kg/s
SEC	Specific electric energy consumption, kW_e/ kW_{th}
SWC	Specific water consumption, L/h· kW_{th}
T_{amb}	Ambient temperature, ºC
TL	Thermal load, %
$\boldsymbol{wc}$	Water consumption, L/h
$\boldsymbol{wc_{HC}}$	Water consumption in a hybrid configuration, L/h

wc_{WC}	Water consumption in only-wet configuration, L/h
λ_{cond}	Latent heat of condensation, kJ/kg

Abbreviations

ACC	Air Cooled Condensers
ACHE	Air Cooler Heat Exchanger
CIEMAT	Centro de Investigaciones Energéticas, Medioambientales y Tecnológicas
CSP	Concentrated Solar Power
DC	Only-dry
VFD	Variable Frequency Drive
HC	Hybrid cooling
HCT	Hybrid cooling tower
PID	Proportional, Integral and Derivative control
PLC	Programmable Logic Controller
PSA	Plataforma Solar de Almería
P25	Parallel with a split ratio of 25%
P50	Parallel with a split ratio of 50%
P75	Parallel with a split ratio of 75%
SS	Series
WASCOP	Water Saving for Concentrated Solar Power

WC	Only-wet
WCT	Wet Cooling Tower

Credit author statement

Patricia Palenzuela: Conceptualization, Methodology, Formal analysis, Investigation, Writing - Original Draft **Lidia Roca**: Conceptualization, Methodology, Formal analysis, Investigation, Writing - Original Draft **Faisal Asfand**: Conceptualization, Writing - Review & Editing **Kumar Patchigolla**: Conceptualization, Writing - Review & Editing

Acknowledgments

We thank the Plataforma Solar de Almeria for providing access to its installations

References

[1] K. Damerau, K. Williges, A.G. Patt, P. Gauché, Costs of reducing water use of concentrating solar power to sustainable levels : Scenarios for North Africa, Energy Policy. 39 (2011) 4391–4398. https://doi.org/10.1016/j.enpol.2011.04.059.

[2] S.W. Mohammed Ali, N. Vahedi, C. Romero, A. Oztekin, An optimization for water requirement in natural gas combined cycle power plants equipped with once-through and hybrid cooling systems and carbon capture unit, Water-Energy Nexus. 3 (2020) 117–134. https://doi.org/10.1016/j.wen.2020.08.001.

[3] M. Martín, M. Martín, Cooling limitations in power plants : Optimal multiperiod design of natural draft cooling towers, Energy. 135 (2017) 625–636. https://doi.org/10.1016/j.energy.2017.06.171.

[4] A. Corti, E. Carnevale, Environmental impact from wet plumes in combined-cycle power plants, Appl. Therm. Eng. 18 (1998) 1049–1057. https://doi.org/10.1016/S1359-4311(98)00029-5.

[5] S.K. Tyagi, A.K. Pandey, P.C. Pant, V. V. Tyagi, Formation, potential and abatement of plume from wet cooling towers: A review, Renew. Sustain. Energy Rev. 16 (2012) 3409–3429. https://doi.org/10.1016/j.rser.2012.01.059.

[6] T.M.L. Wigley, P.R. Slawson, The effect of atmospheric conditions on the length of visible cooling tower plumes, Atmos. Environ. 9 (1975) 437–445.

[7] X. Xu, S. Wang, Z. Ma, Evaluation of plume potential and plume abatement of evaporative cooling towers in a subtropical region, Appl. Therm. Eng. 28 (2008) 1471–1484. https://doi.org/10.1016/j.applthermaleng.2007.09.003.

[8] C. Turchi, K. Chuck, Water use in concentrating solar power (CSP), (2009). http://www.swhydro.arizona.edu/renewable/presentations/thursday/turchi.pdf.

[9] A. Colmenar-Santos, D. Borge-Diez, C.P. Molina, M. Castro-Gil, Water consumption in solar parabolic trough plants : review and analysis of the southern Spain case, Renew. Sustain. Energy Rev. 34 (2014) 565–577. https://doi.org/10.1016/j.rser.2014.03.042.

[10] K. Hooman, Z. Guan, H. Gurgenci, Advances in dry cooling for concentrating solar thermal (CST) power plants, Elsevier Ltd, 2017. https://doi.org/10.1016/B978-0-08-100516-3.00009-5.

[11] A. Poullikkas, I. Hadjipaschalis, G. Kourtis, A comparative overview of wet and dry cooling systems for Rankine cycle based CSP plants, Trends Heat Mass Transf. 13 (2013) 27–50.

[12] A.M. Blanco-Marigorta, M. Victoria Sanchez-Henríquez, J.A. Peña-Quintana, Exergetic comparison of two different cooling technologies for the power cycle of a thermal power plant, Energy. 36 (2011) 1966–1972. https://doi.org/10.1016/j.energy.2010.09.033.

[13] C. Kutscher, D. Costenaro, Assessment of evaporative cooling enhancement methods for air-cooled geothermal power plants, No. NREL/CP-550-32394. Natl. Renew. Energy Lab., Golden, CO.(US). (2002) 1–9. http://www.nrel.gov/docs/fy02osti/32394.pdf.

[14] S. He, H. Gurgenci, Z. Guan, K. Hooman, Z. Zou, Comparative study on the performance of natural draft dry, pre-cooled and wet cooling towers, Appl. Therm. Eng. 99 (2016) 103–113. https://doi.org/10.1016/j.applthermaleng.2016.01.060.

[15] H. Zhai, E.S. Rubin, A techno-economic assessment of hybrid cooling systems for coal- and natural-gas-fired power plants with and without carbon capture and storage, Environ. Sci. Technol. 50 (2016) 4127–4134. https://doi.org/10.1021/acs.est.6b00008.

[16] H. Hu, Z. Li, Y. Jiang, X. Du, Thermodynamic characteristics of thermal power plant with hybrid (dry/wet) cooling system, Energy. 147 (2018) 729–741. https://doi.org/10.1016/j.energy.2018.01.074.

[17] S. Taghian Dehaghani, H. Ahmadikia, Retrofit of a wet cooling tower in order to reduce water and fan power consumption using a wet/dry approach, Appl. Therm. Eng. 125 (2017) 1002–1014. https://doi.org/10.1016/j.applthermaleng.2017.07.069.

[18] T. Tang, J. Xu, S. Jin, H. Wei, Study on Operating Characteristics of Power Plant with Dry and Wet Cooling Systems, Energy Power Eng. 05 (2013) 651–656. https://doi.org/10.4236/epe.2013.54b126.

[19] F. Asfand, P. Palenzuela, L. Roca, A. Caron, C.-A. Lemarié, J. Gillard, P. Turner, K. Patchigolla, Thermodynamic performance and water consumption of hybrid cooling system configurations for concentrated solar power plants, Sustainability. 12 (2020) 1–19.

[20] E. Rezaei, S. Shafiei, A. Abdollahnezhad, Reducing water consumption of an industrial plant cooling unit using hybrid cooling tower, Energy Convers. Manag. 51 (2010) 311–319. https://doi.org/10.1016/j.enconman.2009.09.027.

[21] H. Wei, X. Huang, L. Chen, L. Yang, X. Du, Performance of a novel natural draft hybrid cooling tower for thermal power generation, Energy Procedia. 158 (2019) 5231–5237. https://doi.org/10.1016/j.egypro.2019.01.661.

[22] W. Asvapoositkul, M. Kuansathan, Comparative evaluation of hybrid (dry/wet) cooling tower performance, Appl. Therm. Eng. 71 (2014) 83–93. https://doi.org/10.1016/j.applthermaleng.2014.06.023.

[23] M. Deziani, K. Rahmani, S.J. Mirrezaei Roudaki, M. Kordloo, Feasibility study for reduce water evaporative loss in a power plant cooling tower by using air to air heat exchanger with auxiliary fan, Desalination. 406 (2017) 119–124. https://doi.org/10.1016/j.desal.2015.12.007.

[24] A. Chorak, P. Palenzuela, D.C. Alarcón-Padilla, A. Ben Abdellah, Experimental characterization of a multi-effect distillation system coupled to a flat plate solar collector field: Empirical correlations, Appl. Therm. Eng. 120 (2017) 298–313. https://doi.org/10.1016/j.applthermaleng.2017.03.115.

[25] B.N. Taylor, C.E. Kuyatt, Guidelines for evaluating and expressing the uncertainty of NIST measurement results, 1994. http://physics.nist.gov/TN1297.